# Flexural strength of roller compacted concrete pavements reinforced with glass-roved textiles

## Morteza Madhkhan[*1], Saeid Nowroozi[1] and Mohammad E. Torki[2a]

[1]*Department of Civil Engineering, Isfahan University of Technology, Isfahan, 8415683111, Iran*
[2]*Department of Aerospace Engineering, Texas A&M University, College Station, TX 77843, USA*

**Abstract.** The one-way (two-way) flexural strength of RCC prisms (circular slabs) reinforced with glass fiber textiles is addressed. To this end, alkaline-resistant glass fiber textiles with three surface weights were used in the composite, the matrix concrete was designed with zero/nonzero slump, and the textiles were used with/without an intermediate layer provided by epoxy resin and sand mortar. Prisms were tested under a four-point loading apparatus and circular slabs were placed on simple supports under a central load. Effects of the amount and geometry of reinforcement, matrix workability, and the intermediate layer on the ultimate load and deflection were investigated. Results revealed that, with a specific reinforcement amount, there is an optimum textile tex for each case, depending on the matrix mix design and the presence of intermediate layer. Similar results were obtained in one-way and two-way bending tests.

**Keywords:** RCC pavements; TRC; glass fiber textile; flexural strength

## 1. Introduction

*Roller Compacted Concrete* (RCC) is exclusively remarked for its enhanced toughness, rapid construction, and economic advantage. Although RCC used to have rough surface thus limited to low-speed pavement, recent improvements in construction equipment and techniques have further facilitated the use of this material in high-speed pavement (Dobrowolsky 1998). Hence, RCC can presently be used in numerous fields including storage enclosures, routes, airplane hangars, slope preservation in embankments and soil dams, floors in heavy-industry factories (Delatte *et al*. 2003), and quite recently, even in large storage dams with special design considerations (Ashtankar and Chore 2014). In general, the mechanical behavior of RCC is similar to that of ordinary concrete, but the mechanical *properties* of RCC, including compressive strength, flexural strength, shear strength, and toughness, have proven higher (Tayabgi and Okamoto 1998, Piarc 1993, Tricbes 1998). In particular, due to its great energy absorption, i.e., ductility, it has recently been extensively utilized in wharfs, terminals, and airports (ACI 325.10R-99 2004, Logie and Oliverson 1987). On the other hand, its physical characteristics, including durability and water absorption, are better than, or at least as good as, those of ordinary concrete. For instance, it has

---

∗Corresponding author, Associate Professor, E-mail: madhkhan@cc.iut.ac.ir
[a]E-mail: mtorki@tamu.edu

proven effective against freeze and thaw, and it has been said to have less water absorption than ordinary concrete, esp. with the use of silica fume (Piarc 1993, ACI 325.10R-99 2004, Holder 1984, Banthia *et al.* 1992). Owing to its high porosity, high flow rates of water would safe-keep RCC roads in heavy rains and would preclude damage induced by freeze and thaw. The main downside within RCC, however, stems from its high porosity. That is, pervious concrete mixture containing little or no sand, creates a substantial void content. High porosity, added to low mortar content, reduces the concrete strength relative to conventional concrete mixtures whereas sufficient strength for many applications is readily achieved (Piggot and Eng 1999, Tennis *et al* 2004).

In order to have more ductility, resistance against fatigue, and tensile strength, as well as to reduce cracks and design thickness of the pavement, it is inevitable to reinforce RCC pavements. There are several ways to do this, including the use of steel or polypropylene fibers and textile reinforcement. Among all, TRC (*Textile Reinforced Concrete*) combines the virtues of fiber-reinforced and bar-reinforced concrete, including high compressive, flexural, shear, and abrasion resistance as well as light weight, cost effectiveness, and more construction speed. Moreover, textile nets need not be covered by concrete to prevent corrosion. Its major applications include façade elements, rhombic frameworks, and barrel-shaped shells (Hegge and Voss 2008). Studies demonstrate that first-generation glass fiber-reinforced polymer bars are not proper structural reinforcing elements in concrete members in that they easily lose durability in alkaline environments, especially at stress levels of 15% or higher (Sen *et al.* 2002, Bentur *et al.* 2006). Even for early alkali-resistant glass products, long-term weathering tests on first-generation glass fibers had revealed that reinforced concrete panels reinforced with those AR fibers might exhibit long-term reduced tensile strength and loss of ductility (Shah *et al.* 1988). Upon experiment, however, a few recently-produced glass fiber products have proven highly resistant against alkaline settings. Any of these registered types of glass fibers can be employed in RCC pavements provided sufficient concrete cover exists around the fibers (ACI 544.1R-96 2004). These glass fibers are mostly known as AR glass fibers, so named as to be Alkali-Resistant. The alkali resistance of AR glass fibers takes place majorly as a result of adding zirconium oxide, and most highly-valued fibers are known to have zirconia contents of 19% or higher. AR glass fibers have proven highly efficacious in controlling restrained shrinkage cracking of concrete. AR glass fibers are known to promote multiple micro cracking and reduce major crack widths. Accordingly, introduction of glass fibers improves the flexural strength and ductility, and subdues the negative impacts of exposure to elevated temperatures. Even rather low mass fractions of AR glass, e.g., 1%, are highly contributive towards enhancement of material properties (Mirza and Sorooshian 2002, Cem-FIL 2015). Moreover, the acid resistance of AR glass fibers has proven as equally high as its alkali resistance (Wei *et al.* 2010).

Hence, newly manufactured glass products should be utilized to avert premature loss of strength. Even in the latter, alkaline ions and moisture can diffuse from outside through the cracks and voids to the interphases and reach the fibers. Adequate cover should thus be provided to forestall corrosion (Benmokrane *et al.* 2002, Wei *et al.* 2010).

Many investigations on RCC pavements reinforced with fibers have been reported in the literature. Kagaya *et al.* (2001) used steel fibers with two different lengths and shapes to investigate the effect of fibers on the segregation of aggregates, mechanical properties, and freeze-and-thaw resistance of RCC pavements. They observed that the segregation of coarse aggregates is lower with the presence of fibers. The mechanical properties, including toughness and flexural strength as well as freeze-and-thaw resistance of RCC pavements proved to be higher than those in

RCC without fibers. Angelakopoulos *et al*. (2009) studied the effect of steel fibers on the flexural strength and toughness of RCC pavements. They deduced that, with a constant amount, longer fibers, esp. longer than 50 mm, add to the stability of the load-deflection behavior. Madhkhan *et al*. (2011, 2012) assessed the effects of pozzolans as well as steel and polypropylene fibers on compressive and flexural strengths as well as toughness and energy absorption of RCC pavements. They concluded that steel fibers alone don't bear a considerable effect on the rupture modulus, but they increase the rupture modulus when used with high amounts of pozzolans (e.g., 30%). Moreover, steel fibers increase toughness indices and energy absorption. However, neither the rupture modulus nor the toughness indices are affected by polypropylene fibers. Xu and Hannant (1992) discussed the flexural behavior of cement mortar composites containing a combination of polypropylene nets with glass strands and roving. They gathered that the combination of polypropylene and glass fibers involves a better interaction between the two phases and increases the proportionality limit and improves the post-cracking flexural behavior of the composite. Also, it has been noticed that using woven glass roves can increase toughness up to 80 percent (Griffiths and Ball 2000). On the basis of experiments performed on concrete beams reinforced with glass textiles, Hegger and Voss (2008) extracted a formula expressing that the flexural load capacity of the composite is dependent on the geometry of the roves, the penetration depth of the matrix phase inside the rove, and the interconnection between the textile fibers. Finally, Weithold and Hojczyk (2009) concluded that, to have a better structural behavior, esp. after initial cracking, the textile should have a greater number of roves with smaller cross sections rather than a smaller number of roves with larger cross sections.

As stated above, many research works have been carried out concerning the use of fibers in RCC. However, meagre work on the application of glass textile in reinforcing RCC pavements is reflective of the impending need to more extensive research in this field. The present work addresses the flexural strength of TRC reinforced with a new generation of glass fiber roves, including one-way bending in prisms and two-way bending in circular slabs. Research objectives are to seek the effects of textile geometry on the flexural behavior, and suggesting a way to improve the flexural effect of textile reinforcement. Results can be used as benchmark.

## 2. Textile-Reinforced Concrete (TRC)

*Textile Reinforced Concrete* (TRC) is a composite material at least consisting of two phases: the reinforcing phase (increasing the mechanical properties) and the matrix phase (acting as to keep the whole material stably in shape). A third phase, known as the intermediate phase, can be also included, functioning as an improvement for the matrix behavior. The reinforcing phase contains one or more woven nets including synthetic fibers made of carbon, aramid or glass. Due to more availability, glass fibers are cheaper than other kinds of fibers.

Thanks to its enhanced physical and mechanical advantages, Cem-FIL is now one of the most widely used items among all well-known AR products. Included in the benefits of Cem-FIL in comparison to other glass fibers are good compatibility with cement matrix, better workability even at high dosage, increased chemical resistance (due in part to deicing products), extended long-term durability of concrete, resistance against air permeability, as well as fast and uniform dispersion throughout the concrete mixture (Cem-FIL, 2015).

The properties of the glass fiber used in the present research, which conforms well to all duration standards (including alkaline resistance), are given in Table 1. The textile can be roved at

Table 1 Properties of glass fibers used in the present research

| Specimen's code | Textile grade (tex) | | Number of string (in 25 mm) | | Surface weight (g) | Tensile strength (MPa) | |
|---|---|---|---|---|---|---|---|
| | Warp | Woof | Warp | Woof | | Warp | Woof |
| 125 | 528 | 528 | 41031 | 41031 | 125 | >11 | >11 |
| 135 | 264 | 264 | 5 | 5 | 135 | >13 | >13 |
| 200 | 528 | 2×264 | 40981 | 40981 | 200 | >22 | >9 |
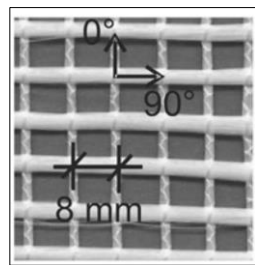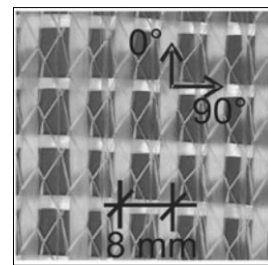


(a)                    (b)

Fig. 1 Illustrations of roved textiles: (a) tricot, (b) chain
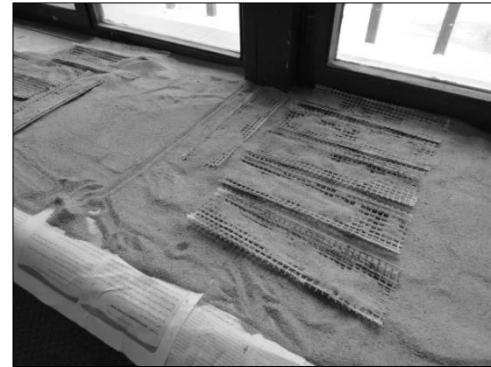


Fig. 2 The way of introducing the intermediate layer

right or diagonal angles, as shown in Fig. 1.

The matrix phase is a finely-granulated concrete containing 0-1 *mm* aggregates to provide utmost adhesion with the textile and pass the textile pores leaving the fewest voids. The cement used in the present research is Portland Type (I). For the sake of contrast, two mix designs are used in this phase. In the first one, named as C11, the *w/c* ratio is 0.33, which facilitates the compaction of RCC because of its zero slump. In the second one, named as C1, the *w/c* ratio is 0.4, which produces a self-compacting capability for the composite, it increases the contact surface with the textile, and thus the tensile strength of the composite will be improved. The different effects of these two matrix mix designs will be investigated in the forthcoming sections.

The intermediate phase in this research is provided by impregnating textile roves with epoxy resin and then immersing the roves in a mortar made of very fine (i.e., 0-1 mm) grains, as shown in Fig. 2. After this assemblage has been set, it can be used in fresh concrete.

Table 2 Physical properties of coarse aggregates

| Standard | Physical property | |
|---|---|---|
| ASTM C136 | Maximum size | 19 mm |
| ASTM C29 | Compacted dry density | 1580 kg/m$^3$ |
| ASTM C127 | Specific gravity | 2.72 |
| ASTM C566 | Natural moisture | 0 |
| ASTM C127 | Saturated dry-surface water absorption (%) | 0.6 |
| ASTM C131 | Los Angeles percentage | 24 |

Table 3 Physical properties of fine aggregates

| Standard | Physical properties | |
|---|---|---|
| ASTM C128 | Specific gravity | 2.4 |
| ASTM C566 | Natural moisture | 2 |
| ASTM C128 | Saturated dry-surface water absorption (%) | 1.4 |
| ASTM C136 | Fineness modulus | 3.62 |
| ASTM D2419 | Sand equivalent (%) | 78 |
| ASTM C117 | Percentage passed from #200 | 3.8 |
| ASTM D4318 | Plasticity index | NP |

## 3. Mix design

The mix design proposed for RCC differs from that of ordinary concrete in that the mixture normally does not contain aerators, and it feels drier since it demands more fine aggregates (to have more convenience for compaction), and the maximum nominal diameter of aggregates must be limited to 19 mm to minimize segregation and provide as smooth a surface as possible (ACI 325.10R-99 2004, Hansen and Reinhard 1991). The mix designs in the present research are proposed on the basis of the *soil approach*, in which dry density is plotted against the moisture of compacted concrete, and the mix design pertaining to the maximum dry density is considered as the final alternative. This approach is mostly used for rather small thicknesses, as in pavements and slabs (ACI 325.10R-99 2004, ACI 211.3R-02 2004). The concrete mixture consists of the following materials.

### 3.1 Coarse and fine aggregates

As stated above, the maximum nominal diameter of aggregates must be limited to 19 mm. This diameter is proper for 150×150×150 mm cubic and 350×100×100 mm molds since 5 times the maximum nominal diameter of aggregates must be smaller than the minimum mold side (ASTM C33-03 2004). The physical properties of coarse aggregates used in the present research are included in Table 2.

The fine material used in the present research is natural sand, the physical properties of which are included in Table 3.

The granulation of aggregates in the final mix design has been considered as 70 percent fine and 30 percent coarse aggregates, which conforms well to the upper and lower bounds recommended by ACI 325.10R-99 (ACI 325.10R-99).

Table 4 The granulation of RCC in the present work

| Sieve size (mm) | | 25 | 19 | 12.5 | 9.5 | 4.75 | 2.36 | 1.18 | 0.6 | 0.3 | 0.15 | 0.075 |
|---|---|---|---|---|---|---|---|---|---|---|---|---|
| Passed percentage | Lower bound | 100 | 82 | 72 | 66 | 51 | 38 | 28 | 18 | 11 | 6 | 2 |
| | Upper bound | 100 | 100 | 93 | 85 | 69 | 56 | 46 | 36 | 27 | 18 | 8 |
| | Present work | 100 | 99.9 | 89.64 | 73.98 | 56 | 38.5 | 27.79 | 21.42 | 14.7 | 4.7 | 2.6 |
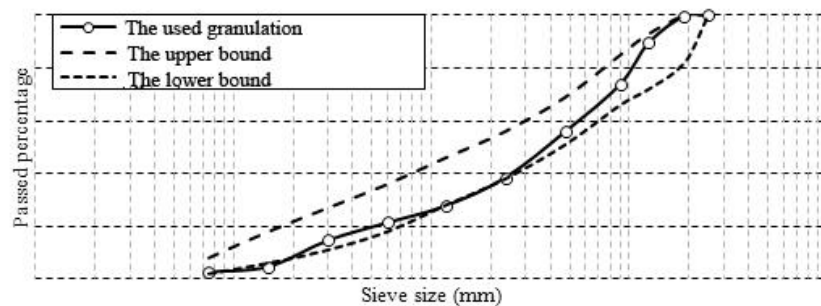


Fig. 3 The granulation of RCC

Table 5 Chemical components of the used pozzolan

| Chemical components | Existing percentage |
|---|---|
| $SiO_2$ | 60-62 |
| $Al_2O_3$ | 17.8-18.5 |
| $Fe_2O_3$ | 4.6-5.5 |
| CaO | 6.5-7.1 |
| MgO | >2.3 |
| $SO_3$ | >0.2 |
| Cl | >2.5 |
| $K_2O$ | >2.0 |

The complete granulation scheme of the present mix design is tabulated in Table 4 and shown in Fig. 3. To be more specific, typical crushed limestone was used as gravel, and silicon as well as fine limestone (smaller-than-5 mm diameter) was taken as the sand part.

### 3.2 Cementitious materials

The amount of cementitious materials in the soil approach is considered as some percentage of the total aggregates' amount, which is suggested between 12 and 17 percent by many researchers. The cementitious materials in the present research include cement (Portland Type I) and natural pozzolan, which is included as 20 percent of the cement weight. The chemical components of this natural pozzolan are given in Table 5.

### 3.3 Water

The optimum water content is obtained based on the physical properties of the aggregates and
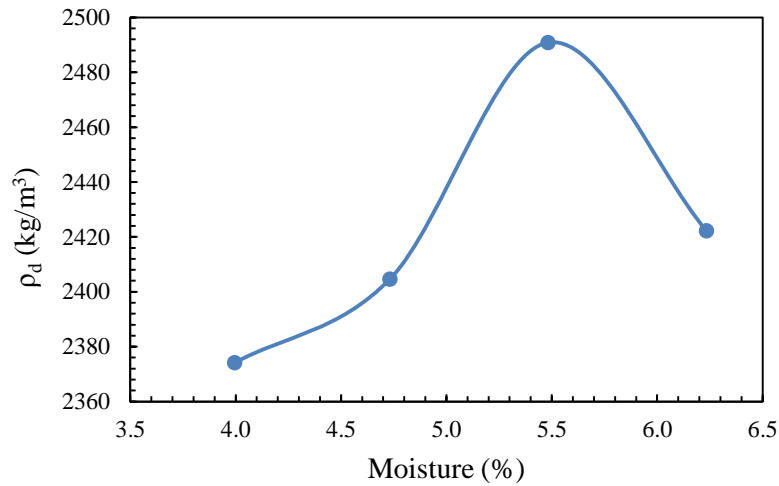
Fig. 4 Evolution of dry density as function of moisture content. The optimum moisture, associated with the maximum dry density, is almost 5.5%

Table 6 RCCP mix design

| Specimen code | Cement | Pozzolan | Gravel (10-10 mm) | Gravel (5-10 mm) | Sand (0-5 mm) | Water |
|---|---|---|---|---|---|---|
| RCCP | 201.1 | 50.28 | 193.31 | 386.62 | 135.28 | 121.72 |

the amount of cementitious materials. More or less water reduces the strength of the design. Fig. 4 illustrates the evolution of dry density vs moisture content. The optimum moisture can be observed as around 5.5%, corresponding to a 2490 kg/m$^3$ dry density.

The final mix design used in the present research, known as the RCCP design, is given in Table 6.

## 4. Test specimens

The test specimens were made in four dimensions: 150×150×150 mm cubic specimens were made for the 28-day compressive strength of RCC, 50×50×50 mm cubic specimens were made for the 28-day compressive strength of the TRC matrix, 350×100×100 mm prismatic specimens were considered for the one-way flexural strength of TRC composites (by applying the four-point loading test according to ASTM C1018), and 600 (diameter)×100 (thickness) mm circular ones were considered for two-way flexural strength of TRC composites (by applying the load on the center point). Concrete was placed and compacted in three 50 mm layers in 150×150×150 mm specimens, two 50 mm layers in prismatic and circular specimens, and one layer in 50×50×50 mm ones, in which it was placed in one layer and compacted with a rod. Each specimen was made in 3 numbers. A Glass textile can mainly undergo tension, thus its name "textile". Hence, it was placed merely at the lowermost layer, i.e., in the tensile block of the cross section. However, as exhibited in Fig. 8, the fractured specimen has been reverted to have more convenience seeing the textile layer after fracture. Textiles were used with three weights per square meter, known as *tex*: 125, 135, and 200 g/m$^2$. Prismatic and circular TRC specimens were made with and without the
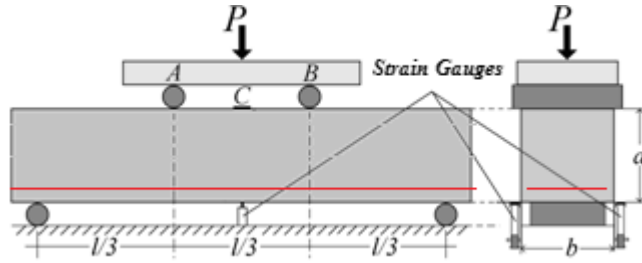
Fig. 5 The four-point flexural test put forward in ASTM C1018 (the textile layer is shown in red color)

intermediate layer. All specimens were demolded after 24 hours, cured in cool water for 28 days, and were then tested after 34 days.

The Kango hammer, with a 750 W power, a 46 cm height, a 7.5 kg weight, exerting 2750 percussions per minute, was used to compact the specimens (Madhkhan *et al*. 2012). Rectangular and circular percussion heads were used to make noncircular and circular specimens, respectively. The mean compressive strength of RCCP, C11, and C1 TRC mix designs were obtained 35.2, 49.4, and 40.6 MPa, respectively.

## 5. One-way flexural behavior

As it was pointed out in section 4, the one-way bending of TRC prisms was evaluated in accordance to ASTM C1018 (ASTM C1018-97 2004), in which the four-point loading test, as indicated in Fig. 5, has been clarified such that the rupture modulus is defined according to Eqs. (1a) and (1b), the former pertaining to the case rupture occurs within the middle one third of the supported length and the latter is for when rupture happens outside the middle one-third of the supported extent, but lies within a distance less than 5 percent of the supported length in relation to the middle one-third of the prism.

$$R = \frac{PL}{bd^2} \tag{1a}$$

$$R = \frac{3Pa}{bd^2} \tag{1b}$$

where $R$ is the rupture modulus, $P$ is the rupture load in kilograms (1 kg≈10 N), $L$ is the specimen's length placed between the two supports in millimeters, and $b$ and $d$ are the specimen's width and height, respectively. In case fracture takes place outside the middle one-third, and lies outside the distance equating 5 percent of the supported length in relation to that area, the specimen will be invalid.

ASTMC78 and ASTMC1018 have considered $b$ and $d$ to be one-third of the supported length (ASTM C1018-97 2004, ASTM C78-02 2004). To properly measure the deflection, two strain

gauges were placed on the two sides of the specimen's cross section, and the deflection was obtained by averaging the values measured at the middle minus the average of those placed at the supports' locations. In this research, a triaxial testing apparatus known as *Triset 50* was used, applying a maximum load of $50 \times 10^3$ N. The loading speed was taken to be 0.0016 mm/sec according to ASTMC1018, and its direction was perpendicular to the concrete casting surface.

The properties of one-way flexural specimens and their test results, including the mean rupture moduli as well as ultimate loads and deflections, are included in Appendix A.

The results can be explained as follows:

### 5.1 Effect of reinforcement amount

Results indicate that textiles have a significant effect on the rupture modulus. The maximum effect (44.5% increase) has occurred in E5L125gC1 since this effect is dependent upon the tensile strength of the textile, which is itself function of the matrix, the number of fibers and layers, and the adhesion between the textile and matrix. All specimens were ruptured in the middle one third.
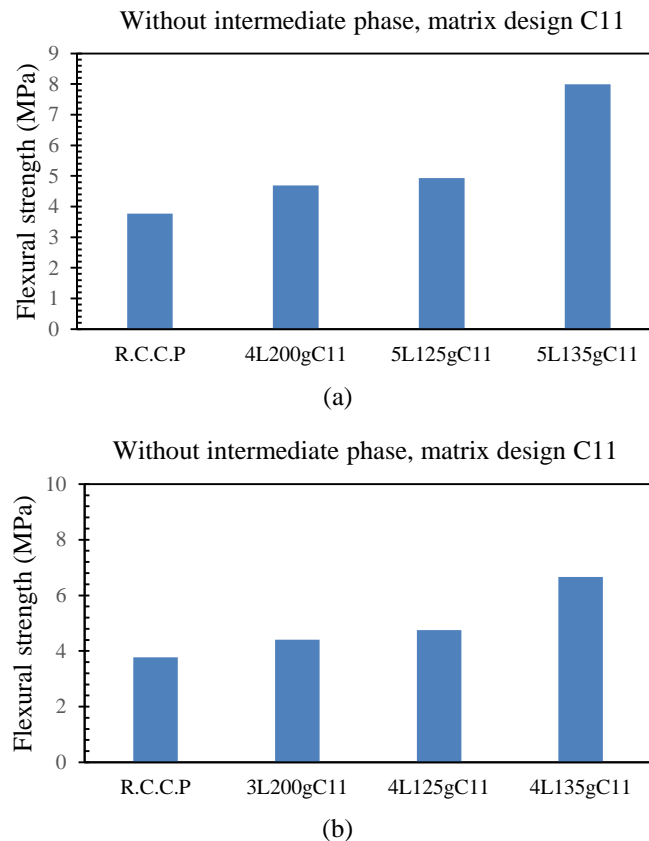


(a)



(b)

Fig. 6 Effect of the textile geometry on the flexural strength of prismatic specimens all equally reinforced (except the RCCP specimen): (a,b) without intermediate phase, matrix design C11; (c,d) without intermediate phase, matrix design C1; (e,f) with intermediate phase, matrix design C11; and (g,h) with intermediate phase, matrix design C1
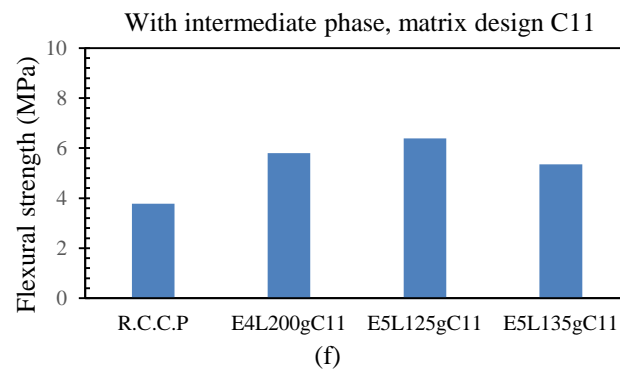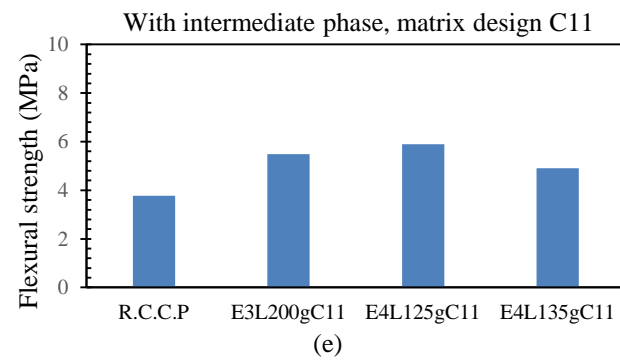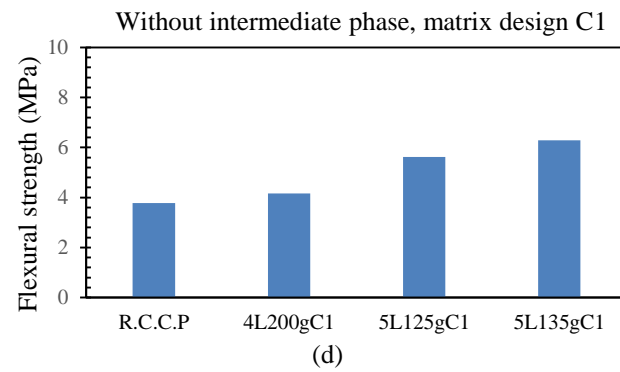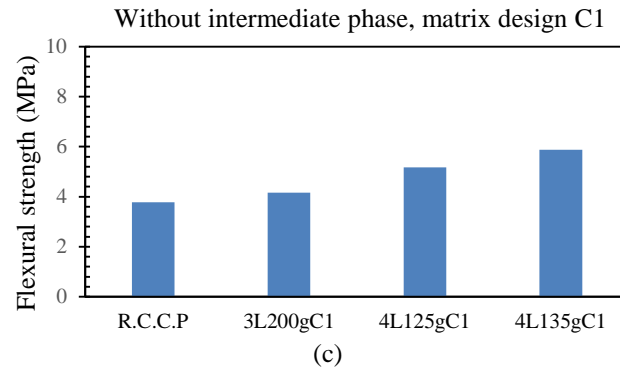
Without intermediate phase, matrix design C1



(c)

Without intermediate phase, matrix design C1



(d)

With intermediate phase, matrix design C11



(e)

With intermediate phase, matrix design C11
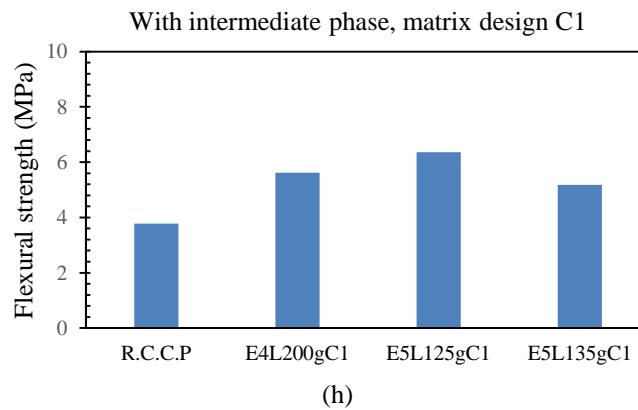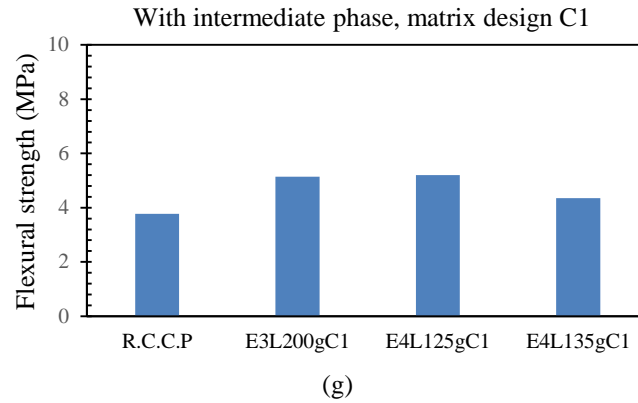


(f)

Fig. 6 Continued

(g)



(h)

Fig. 6 Continued

Cracking was initiated in the tensile region, and fracture occurred when one of these cracks spread to the compressive region.

Likewise, textiles have a considerable effect on the ultimate load and deformation, i.e. ductility. The utmost effect on these two quantities (almost 113% increase) has occurred in 5L135C11.

### 5.2 Effect of textile geometry (tex)

In order to evaluate this effect, specimens with equal reinforcement amounts have been gathered together and compared. Figs. 6 and 7 indicate this comparison for ultimate loads and deflections, respectively.

Fig. 6 demonstrates that, with identical reinforcement amounts, the ultimate load is higher in specimens containing 125 g textiles in composites with zero-slump (non-workable) matrix. This lies in the fact that, in a specific reinforcement amount, increasing the size of meshes (i.e., decreasing the cross section of roves) and increasing the number of layers at the same time helps the matrix to better penetrate into the roves. In this case, the textile will be completely fractured in tension, whereas it will be scaled off from the matrix when the mesh size is too small, as in the 200 g textile.

However, as demonstrated in Fig. 7, with identical reinforcement amounts, the ultimate deflection is higher with 135 g textiles in composites with nonzero-slump (self-compacting)
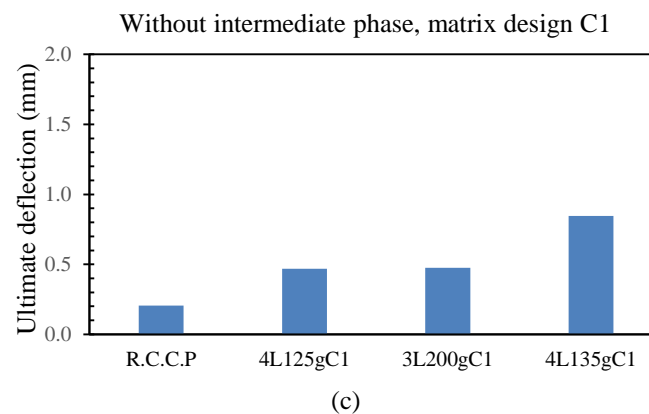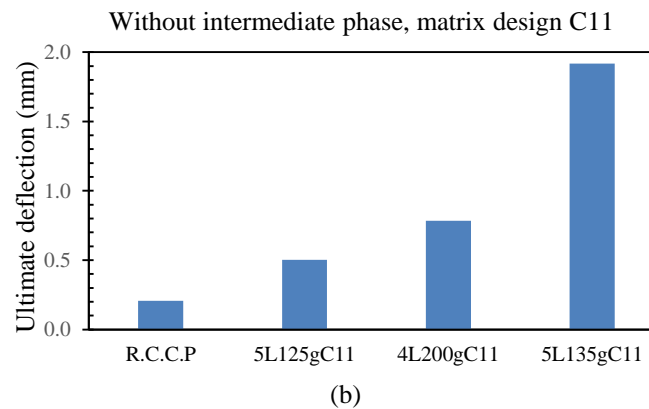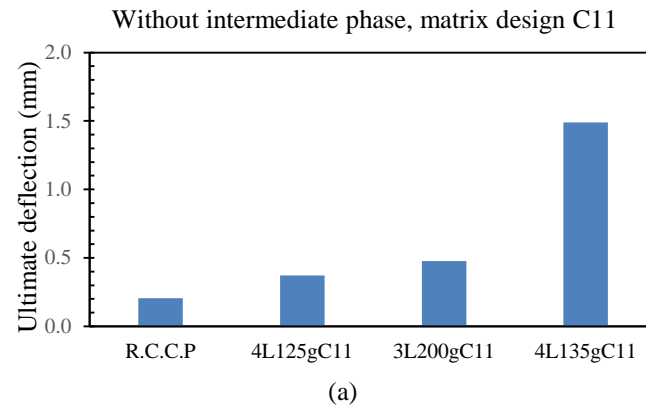


(a)



(b)



(c)

Fig. 7 Effect of the textile geometry on the ultimate deflection of prismatic specimens all equally reinforced (except the RCCP specimen): (a,b) without intermediate phase, matrix design C11; (c,d) without intermediate phase, matrix design C1; (e,f) with intermediate phase, matrix design C11; and (g,h) with intermediate phase, matrix design C1

matrix. The reason is that, in this case, rather than the mesh size, increasing the number of roves in a specific distance increases the contact surface with the workable matrix concrete. The fracture patterns of the 125, 135, and 200 *g* textiles are compared in Fig. 8.
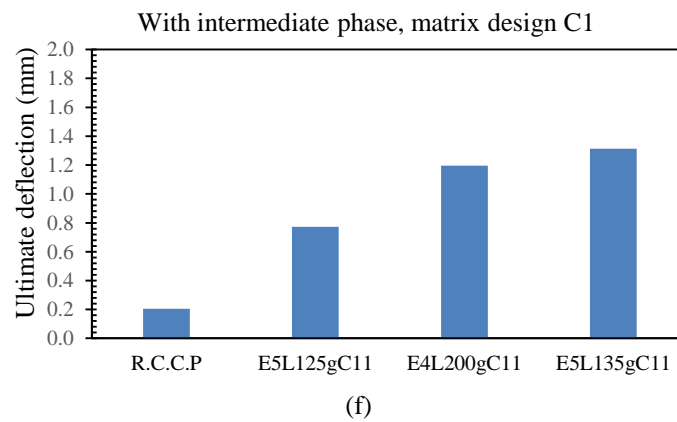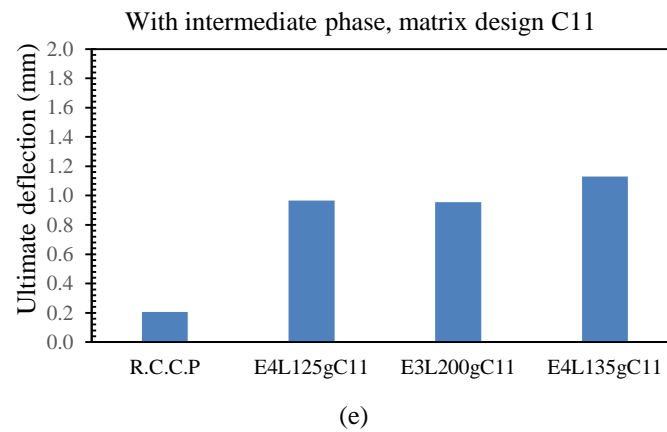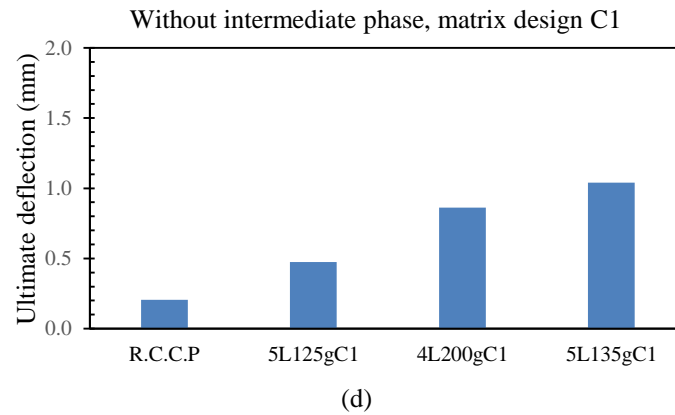
Without intermediate phase, matrix design C1



(d)

With intermediate phase, matrix design C11



(e)

With intermediate phase, matrix design C1



(f)

Fig. 7 Continued

(g)



(h)

Fig. 7 Continued



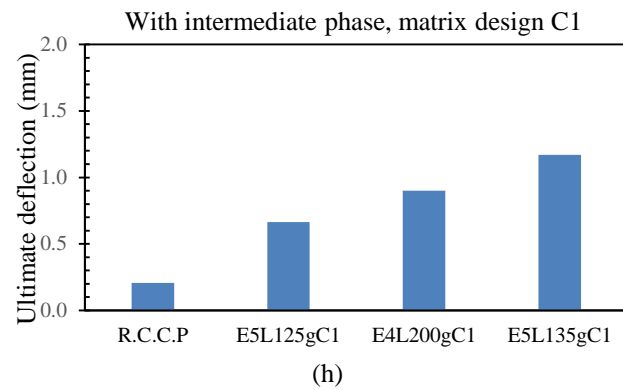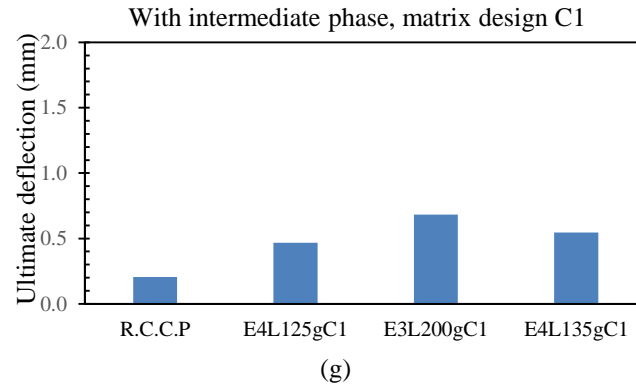| (a) | (b) | (c) |
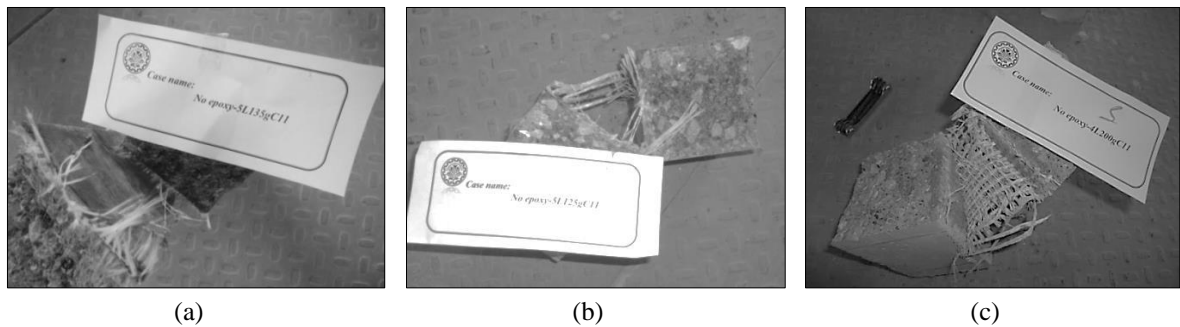
Fig. 8 Comparison of the fracture patterns belonging to: (a) 5L135gC11, (b) 5L125gC11, and (c) 4L200gC11

## 5.3 Effect of the intermediate layer

Fig. 9 shows the effect of the intermediate layer on the ultimate load. The results for the ultimate deflection are similar (Fig. 10 shows an instance).

It can be observed that the intermediate layer has a major effect on the ultimate load and deflection in specimens containing 125 and 200 g textiles. This lies in the fact that, in both types,

the finely-granulated matrix contacts better with the roves, thus the tensile strength of TRC will be increased, and the assemblage will have more ductility, with greater ultimate load and higher ultimate deflection. The fracture patterns of the specimen with 125 g textile with and without the intermediate layer are shown in Fig. 11.



Fig. 9 Effect of the intermediate layer on the flexural strength, all equally reinforced (except the RCCP specimen): (a,b) with/without intermediate phase, matrix design C11; (c-e) with/without intermediate phase, matrix design C1

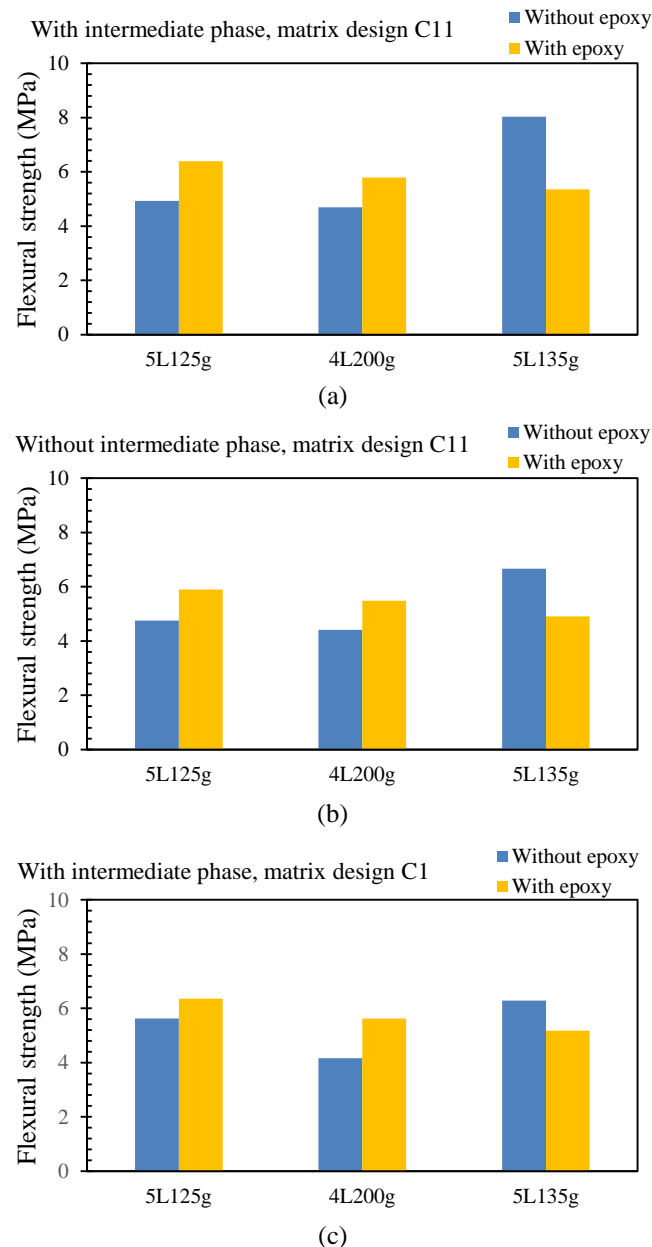Without intermediate phase, matrix design C1



(d)

Without intermediate phase, matrix design C1



(e)
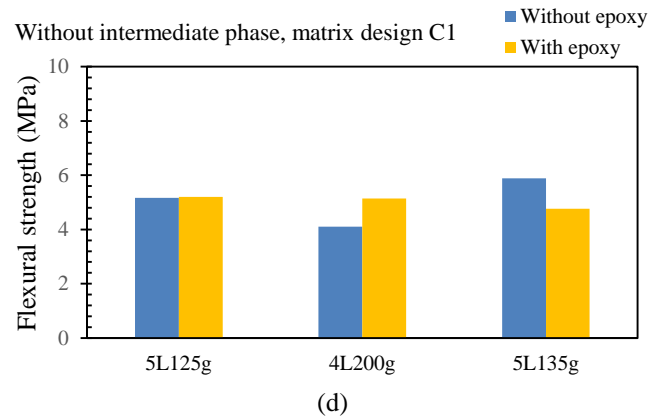
Fig. 9 Continued



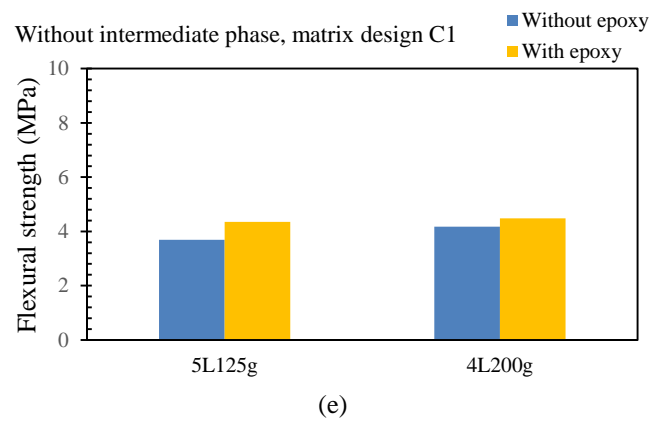Fig. 11 Comparison between the fracture patterns belonging to E5L125gC11 (with the intermediate layer) and 5L125gC11 (without the intermediate layer)

However, for specimens with 135 *g* textiles, the intermediate layer induces a negative effect because the mesh size is small, and thus sand mortar obstructs complete penetration of the concrete matrix into the roves. Fig. 12 confirms this reasoning.

Fig. 12 The fracture pattern belonging to E4L135gC1.



(a)



(b)

Fig. 13 Effect of the matrix mix design on the flexural strength: (a) without the intermediate layer, (b) with the intermediate layer

## 5.4 Effect of matrix mix design

Fig. 13 shows the effect of matrix mix design on the ultimate load. The results for the ultimate

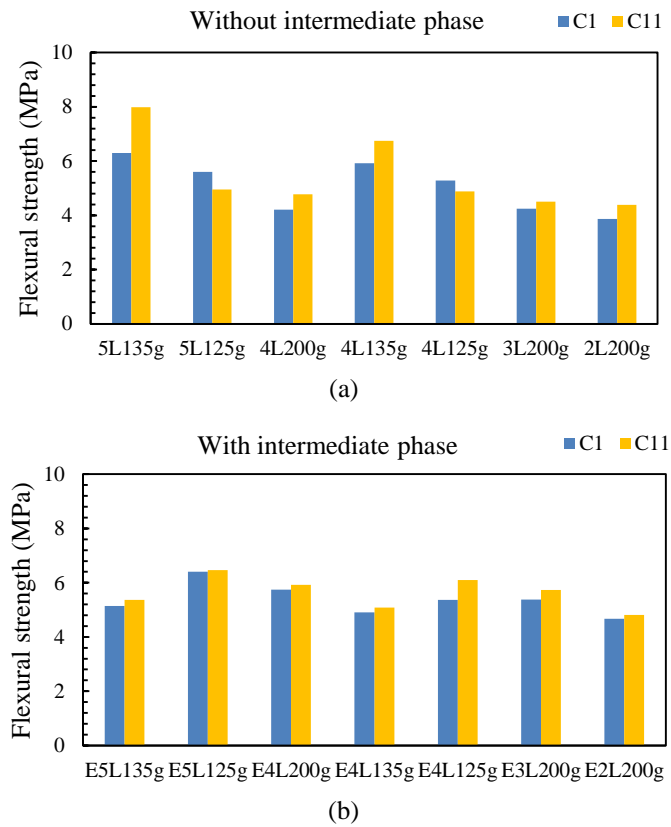deflection are similar. As indicated by this figure, in almost all specimens, reduction in matrix workability leads to a higher ultimate load and deflection owing to the fact that, when RCC is being compacted, a more workable matrix becomes mixed with the main RCC. This would, in fact, enfeeble the whole composite, and it will have less ductility.

The only exception to this deduction is specimens with 125 g textiles in composites without intermediate layers, in which the mesh size is maximal, and thus, by increasing workability of the matrix, the contact surface between the matrix and textile increases to the extent that compaction cannot disorder this contact.

## 6. Two-way flexural behavior

As previously pointed out, the two-way bending of TRC composites was tested with circular slabs with 600 mm diameters and 100 mm thicknesses. They were placed on a simple support and the load was exerted on the center point. The deflection was measured by a gauge placed on the center. The loading speed was, as for other experiments, 0.0016 mm/sec. the schematic and real testing setups are shown in Fig. 14.

The outcomes of two-way bending tests are included in Appendix B. Following are the results being discussed:

### 6.1 Fracture pattern

All specimens were fractured with radial yield lines as depicted in Fig. 14. Fracture occurred together with tensile fracture of textiles.

### 6.2 Cracking load

As observed in Appendix B, textile reinforcement increases the cracking load. The maximum increase in the cracking load has occurred in 5L135C1 (by 33%). The increased cracking load depends on the cracking strength of the TRC composite.
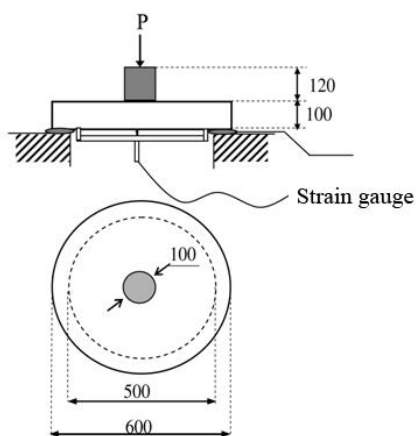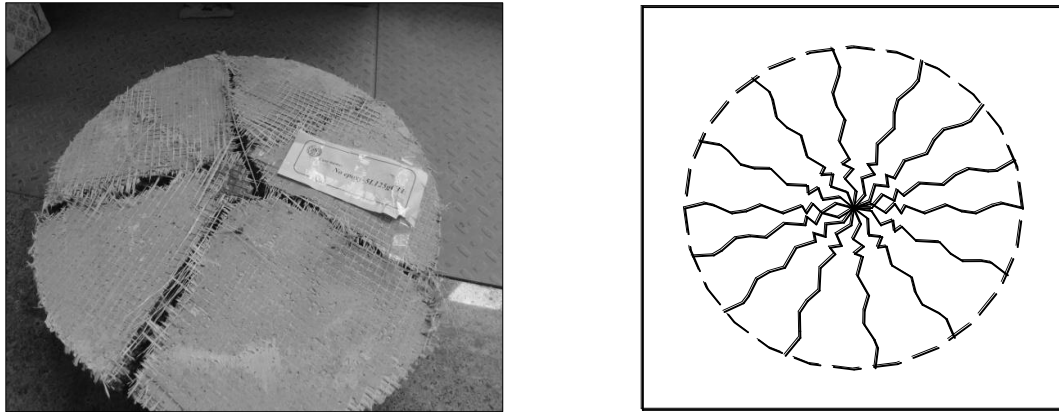


Fig. 14 The testing setup of slabs.

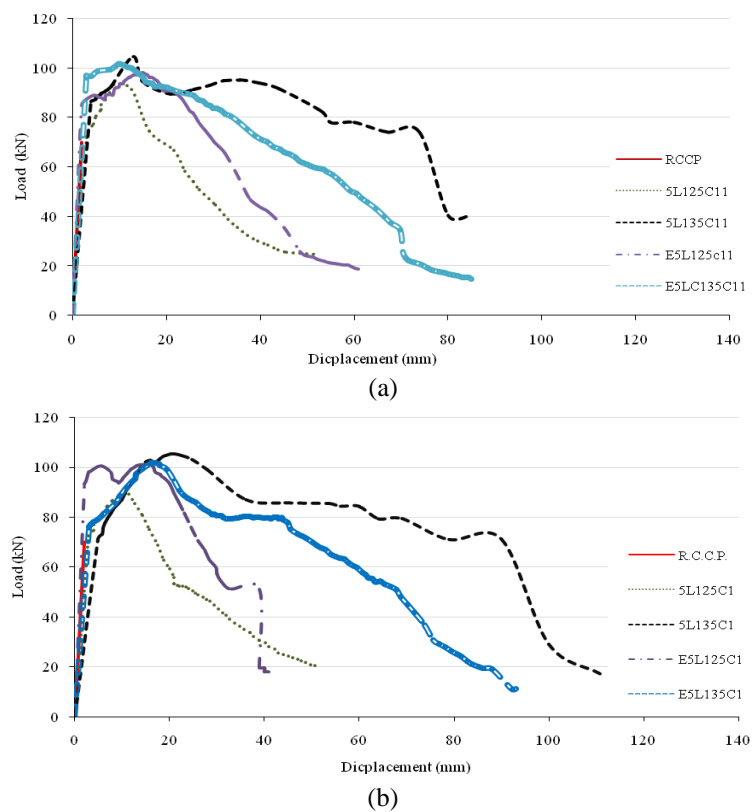Fig. 15 Yield lines on circular slabs.



(a)



(b)

Fig. 16 Load-deflection curves for two-way flexural circular slabs with equal reinforcement: (a) with zero-slump (C11) matrix, and (b) with self-compacting (C1) matrix

## 6.3 Ultimate load and deflection

The load-deflection curves belonging to slab specimens with zero-slump and self-compacting

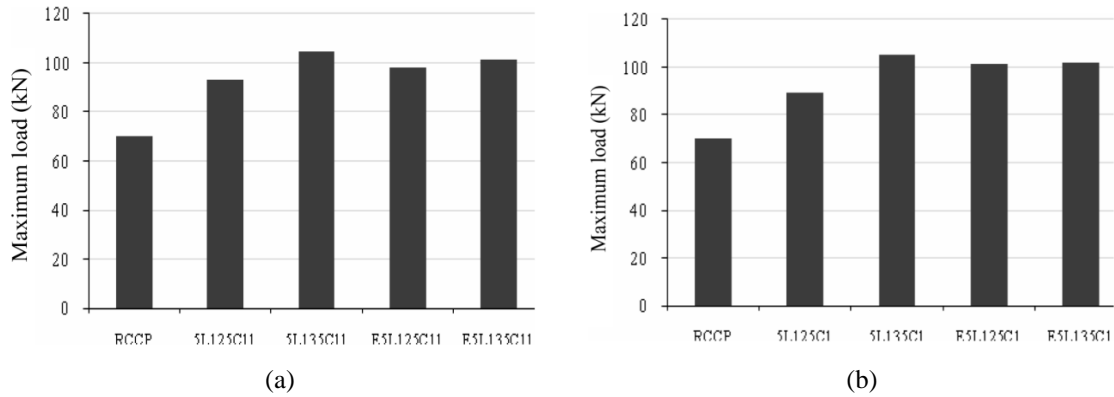(a)                                              (b)

Fig. 17 Comparison of ultimate loads for two-way bending tests (a) with matrix C11, and (b) with matrix C1

matrices are shown in Figs. 16(a) and 16(b), respectively (All plotted curves in each figure have equal reinforcement).

With the same procedure as for one-way bending specimens, results for ultimate loads for equally-reinforced specimens are gathered in separate diagrams in Fig. 17 (with similar results for ultimate deflections). It can be obviously seen that the utmost increase has occurred in 5L135C1 (by 51%).

With full resemblance to one-way bending specimens, with a specific reinforcement amount and matrix mix design, specimens with 135 g textiles have higher ultimate loads and deflections for the same reason clarified in section 5.2, i.e., replacing thicker roves with thinner roves with smaller inter-string distance.

On the other hand, like one-way bending specimens, introducing the intermediate layer has a negative impact on the ultimate load in specimens with 135 g textiles for the same reason stated in subsection 5.3.

Finally, though not as clear as for one-way bending, comparison between specimens, with the only difference in the matrix concrete workability, reveals that increasing matrix workability enfeebles the whole composite.


## 7. Conclusions

The present study deals with the one-way and two-way flexural strength of RCC pavements reinforced with glass-reinforced TRC (textile reinforced concrete). Textiles were used with three surface weights: 125, 135, and 200 g/m$^2$. The RCC mixture was designed according to ACI 325.10R-99 and the matrix was designed as a finely granulated concrete with zero and/or nonzero slump. The textiles were used both with and without an intermediate layer consisting of epoxy resin and sand mortar, where epoxy resin was rubbed around the roving and then the textile was placed in sand mortar. To evaluate the one-way flexural strength, TRC-reinforced RCC prisms underwent the four-point loading test put forward in ASTM C1018, and to measure the two-way flexural strength, a central load was exerted on simply-supported circular slabs. Results include the effects due to the textile geometry, matrix workability, and the intermediate layer with a specific reinforcement amount. It was found that, with a zero-slump matrix, increasing the mesh size leads

to higher strength and ultimate deflection, i.e. ductility. With a specific reinforcement amount and matrix design, specimens with 135 *g* textiles had higher ductility when made without the intermediate layer, while introducing the intermediate layer has a negative impact on these specimens. All the same, with a workable matrix, increasing the number of roves per unit length increases ductility. Finally, in most cases, increasing the matrix workability induced a negative effect on the ultimate load. Similar results were deduced for two-way bending. Identical results were drawn for two-way flexural circular slabs.

## References

ACI 544.1R-96 (2004), "State of the Art Report on Fiber Reinforced concrete", ACI Manual of Concrete Practice, Author, USA.

ACI 325.10R-99 (2004), "State of the Art Report on Roller Compacted Concrete Pavements", ACI Manual of Concrete Practice, Author, USA.

ACI 211.3R-02 (2004), "Guide for Selecting Proportions for No-Slump Concrete", ACI Manual of Concrete Practice, Author, USA.

Ashtankar, V.B. and Chore, H.S. (2014), "Development of design mix roller compacted concrete dam at middle vaitarana", *Adv. Concrete Construct.*, **2**(2), 125-144.

Angelakopoulos, H., Neocleous, K. and Pilakoutas, K. (2009), "Steel fiber reinforced roller-compacted concrete road", *Int. Intersec.*, **6**(1), 45-55.

ASTM C33-03 (2004), "Standard Specification for Concrete Aggregates", Standard Designation C33-03 04.02.

ASTM C1018-97 (2004), "Standard Test Method for Flexural Toughness and First-crack Strength of Fiber Reinforced Concrete (Using Beam with Third Point Loading)", Standard Designation C1018-97 04.02.

ASTM C78-02 (2004), "Standard Test Method for Flexural Strength of Concrete (Using Simple Beam with Third-Point Loading)", Standard Designation C78-02 04.02.

Banthia, N., Pigeon, M., Marchand, J. and Boisvert, J. (1992), "Permeability of roller compacted concrete", *J. Mater. Civil Eng.*, **4**, 27-40.

Benmokrane, B., Wang, P., Ton-That, T., Rahman, H. and Robert, J. (2002),"Durability of glass fiber-reinforced polymer reinforcing bars in concrete environment", *J. Compos. Construct.*, **6**(3), 143-153.

Bentur, A., Ben-Bassat, M. and Schneider, D. (1985), "Durability of glass-fiber-reinforced cements with different alkali-resistant glass fibers", *J. Am. Ceramic Soc.*, **68**(4), 203-208.

Cem-FIL® glass fiber, the solution for concrete reinforcement, 1999-2015 Owens Corning, http://www.cem-fil.com/.

Delatte, N., Amer, N. and Storey, C. (2003), "Improved Management of RCC Pavement Technology", UTCA Report 01231, University Transportation Center for Alabama (UTCA).

Dobrowolsky, J.A. (1998), "Concrete Construction Hand Book: Section 27.2.2. RCC Pavements", McGraw Hill: 27.11-27.20.

Griffiths, R. and Ball, A. (2000), "An assessment of the properties and degradation behavior of glass fiber reinforced polyester polymer concrete", *J. Compos. Sci. Tech.*, **60**(14), 2747-2753.

Guodong, X. and Hannant, D.J. (1992), "Flexural behavior of combined polypropylene network and glass fiber reinforced cement", *J. Cement Concrete Compos.*, **14**(1), 51-61.

Hegge, J. and Voss, S. (2008), "Investigation on the bearing behavior and application potential of textile reinforced concrete", *J. Eng. Struct.*, **30**(7), 2050-2056.

Holder, R. (1984), "Roller Compacted Concrete Pavement Tactical Equipment Hardstand, Line Item 434", Contract No. DACA83-C-0188, Fort Hood, Tex., Fort Worth District, Corps of Engineers.

Kagaya, M., Suzuki, T., Kokubun, S. and Tokuda, H. (2001), "A study of mix proportions and properties of steel fiber reinforced roller-compacted concrete for pavements", *Tran. Proc. JSCE*, **50**(669), 16.

Logie, C.V. and Oliverson, J.E. (1987), "Burlington northern railroad international freight terminal", *Concrete Int. Des. Constr.*, **9**(2), 37-41.

Madhkhan, M., Azizkhani, R. and Torki, M.E. (2011), "Roller compacted concrete pavements reinforced with steel and polypropylene fibers", *Struct. Eng. Mech.*, **40**(2), 149-165.

Madhkhan, M., Azizkhani, R. and Torki, M.E. (2012), "Effects of pozzolans together with steel and polypropylene fibers on mechanical properties of RCC pavements", *J. Construct. Build. Mater.*, **26**(1), 102-112.

Mirza, F.A. and Soroushian, P. (2002), "Effects of alkali-resistant glass fiber reinforcement on crack and temperature resistance of lightweight concrete", *Cement Concrete Compos.*, **24**(2), 223-227.

Piarc Technical Committee on Concrete Roads (1993), The Use of Roller Compacted Concrete for Roads.

Piggott, R.W. and Eng, P. (1999), Roller Compacted Concrete Pavements.

Sen, R., Mullins, G. and Salem, T. (2002), "Durability of E-glass/vinylester reinforcement in alkaline solution", *ACI Structural Journal*, **99**(3), 369-375.

Shah, S.P., Ludirdja, D., Daniel, J.I. and Mobasher, B. (1988), "Toughness durability of glass fiber reinforced concrete systems", *ACI Mater. J.*, **85**(5), 352-360.

Tayabgi, S.D. and Okamoto, P.A. (1987), "Engineering Properties of Roller Compacted Concrete", Transportation Research Record 1136, Transportation Research Board, Washington, D.C..

Tennis, P.D., Leming, M.L. and Akers, D.J. (2004), "Pervious Concrete Pavements (No. PCA Serial No. 2828)", Portland Cement Association, Skokie, IL.

Wei, B., Cao, H. and Song, S. (2010), "Environmental resistance and mechanical performance of basalt and glass fibers", *Mater. Sci. Eng.* A, **527**(18), 4708-4715.

Weichold, O. and Hojczyk, M. (2009), "Size effects in multifilament glass rovings: the influence of geometrical factors on their performance in textile-reinforced concrete", *Textile Res. J.*, **79**(16), 1438-1445.

*CC*

**Appendix A.** Properties and test results of one-way flexural specimens, comprising the mean rupture moduli as well as ultimate loads and deflections.

| Specimen's code[†] | Textile grade (tex) | Number of layers | Matrix design | Reinforcement index[††] (amount) | Rupture modulus (MPa) | Ultimate deflection (mm) | Ultimate load (kN) |
|---|---|---|---|---|---|---|---|
| R.C.C.P. | - | - | - | - | 3.77 | 0.206 | 12.583 |
| 5L135gC11 | 135 | 5 | C11 | 6600 | 4.87 | 1.918 | 26.77 |
| 5L125gC11 | 125 | 5 | C11 | 6600 | 4.34 | 0.503 | 16.45 |
| 4L200gC11 | 200 | 4 | C11 | 6600 | 4.6 | 0.784 | 15.63 |
| 4L135gC11 | 135 | 4 | C11 | 5280 | 3.98 | 1.489 | 22.2 |
| 4L125gC11 | 125 | 4 | C11 | 5280 | 4.64 | 0.372 | 15.83 |
| 3L200gC11 | 200 | 3 | C11 | 5280 | 4.4 | 0.478 | 14.68 |
| 2L200gC11 | 200 | 2 | C11 | 3485 | 4.1 | 0.432 | 13.93 |
| 5L135gC1 | 135 | 5 | C1 | 6600 | 5.01 | 1.039 | 21 |
| 5L125gC1 | 125 | 5 | C1 | 6600 | 5.45 | 0.474 | 18.75 |
| 4L200gC1 | 200 | 4 | C1 | 6600 | 4.03 | 0.863 | 13.88 |
| 4L135gC1 | 135 | 4 | C1 | 5280 | 4.44 | 0.845 | 19.61 |
| 4L125gC1 | 125 | 4 | C1 | 5280 | 4.9 | 0.469 | 17.23 |
| 3L200gC1 | 200 | 3 | C1 | 5280 | 4.1 | 0.475 | 13.67 |
| 2L200gC1 | 200 | 2 | C1 | 3485 | 3.61 | 0.331 | 12.3 |
| E5L135gC11 | 135 | 5 | C11 | 6600 | 4.86 | 1.313 | 17.85 |
| E5L125gC11 | 125 | 5 | C11 | 6600 | 4.67 | 0.773 | 21.3 |
| E4L200gC11 | 200 | 4 | C11 | 6600 | 5.1 | 1.196 | 19.32 |
| E4L135gC11 | 135 | 4 | C11 | 5280 | 4.1 | 1.13 | 16.37 |
| E4L125gC11 | 125 | 4 | C11 | 5280 | 4.46 | 0.966 | 19.65 |
| E3L200gC11 | 200 | 3 | C11 | 5280 | 4.74 | 0.956 | 18.28 |
| E2L200gC11 | 200 | 2 | C11 | 3485 | 4.01 | 0.5 | 14.94 |
| E5L135gC1 | 135 | 5 | C1 | 6600 | 4.4 | 1.17 | 17.26 |
| E5L125gC1 | 125 | 5 | C1 | 6600 | 5.2 | 0.665 | 21.2 |
| E4L200gC1 | 200 | 4 | C1 | 6600 | 5.3 | 0.9 | 18.74 |
| E4L135gC1 | 135 | 4 | C1 | 5280 | 3.9 | 1.006 | 15.87 |
| E4L125gC1 | 125 | 4 | C1 | 5280 | 4.68 | 0.468 | 17.32 |
| E3L200gC1 | 200 | 3 | C1 | 5280 | 4.45 | 0.682 | 17.15 |
| E2L200gC1 | 200 | 2 | C1 | 3485 | 3.76 | 0.546 | 14.5 |

[†]RCCP is the controlling specimen. In other specimens, generally defined as ALBgD, *A* indicates the number of layers, *L* stands for Layers, *B* is the textile code, *g* stands for grams per square meter, and *D* shows the fine concrete matrix code, either C11 or C1. Finally, E demonstrates that the specimen contains the intermediate layer.

[††]The reinforcement index is calculated by multiplying the number of strings, in a 25 mm distance, by the code of the textile, by the number of layers. The reinforcement index indicates the reinforcement amount for the specimen.

**Appendix B.** Results of two-way bending tests.

| Specimen's code | Textile grade (tex) | Number of layers | Matrix design | Reinforcement index | | Cracking load (kN) | Ultimate load (kN) |
|---|---|---|---|---|---|---|---|
| | | | | Warp | Woof | | |
| R.C.C.P | - | - | - | - | - | 69.93 | 69.93 |
| 5L135C11 | 135 | 5 | C11 | 6600 | 6600 | 86.5 | 104.45 |
| 5L125C11 | 125 | 5 | C11 | 6600 | 6600 | 71.89 | 93.17 |
| 5L135C1 | 135 | 5 | C1 | 6600 | 6600 | 71.39 | 105.23 |
| 5L125C1 | 125 | 5 | C1 | 6600 | 6600 | 72.52 | 89.35 |
| E5L135C11 | 135 | 5 | C11 | 6600 | 6600 | 95.5 | 101.5 |
| E5L125C11 | 125 | 5 | C11 | 6600 | 6600 | 84.62 | 98.15 |
| E5L135C1 | 135 | 5 | C1 | 6600 | 6600 | 75.78 | 101.66 |
| E5L125C1 | 125 | 5 | C1 | 6600 | 6600 | 92.9 | 101.1 |

Note: All values are the average value of the three specimens of the same kind.